



COVER SHEET

This is the author version of article published as:

Frost, Ray and Musumeci, Anthony (2007) A spectroscopic and thermoanalytical study of the mineral Hoganite. *Spectrochimica Acta Part A: Molecular and Biomolecular Spectroscopy* 67(1):pp. 48-57.

Copyright 2007 Elsevier

Accessed from <http://eprints.qut.edu.au>

A spectroscopic and thermoanalytical study of the mineral Hoganite

Anthony Musumeci and Ray L. Frost*

Inorganic Materials Research Program, School of Physical and Chemical Sciences, Queensland University of Technology, GPO Box 2434, Brisbane Queensland 4001, Australia.

Abstract

A comprehensive spectroscopic analysis consisting of Raman, infrared (IR) and near infrared (NIR) spectroscopy was undertaken on the newly discovered mineral Hoganite (Copper(II) acetate monohydrate ($\text{Cu}(\text{CH}_3\text{COO})_2 \cdot \text{H}_2\text{O}$)). Assignments of vibrational bands due to the acetate anion have been made in all three forms of spectroscopy. Thermal analysis of the mineral was undertaken to follow its decomposition under a nitrogen atmosphere. Two major mass loss steps at 90 and ~ 220 °C were revealed. These mass losses correspond very well to firstly, the loss of a single water molecule, and then the loss of the acetate anion which quickly decomposes to form carbon dioxide and water.

Key words: Hoganite, copper acetate, Raman spectroscopy, infrared spectroscopy, near infrared spectroscopy, thermal stability

Introduction

The vibrational spectroscopy of acetates in both aqueous media and solid state have been comprehensively studied over a long period of time [1-4]. Though one of the major difficulties associated with studying the spectroscopy of acetates is the large amount of variation in the reported literature [5]. In recent years there has been spectral data published on Mg, Ni, Co, Na and many other metal acetates [1, 6-8] though limited data has been published on copper acetate. One of the reasons for this is the lack of suitable samples. One sample that may be used is a naturally occurring copper acetate known as Hoganite [9].

Copper(II) acetate monohydrate, formally known as the mineral Hoganite, is an interesting metal acetate that is found naturally as bluish green crystals embedded in ferruginous gossan at the Potosi Pit, Broken Hill, New South Wales Australia [9]. Hoganite is found in a monohydrate form as the acetate anion is known to bond to the hydroxyl surface with a 1:1 ratio. Detailed thermogravimetric analysis [10, 11] and X-ray diffraction [9] of the mineral has been published, but to the best of this author's knowledge an in-depth spectral analysis of hoganite has not been documented in the literature. Thus the objective of this work is to determine the Raman, infrared and near infrared spectral characteristics of the mineral Hoganite.

Experimental

Mineral

* Author to whom correspondence should be addressed (r.frost@qut.edu.au)

The mineral Hoganite was obtained from the Potosi Pit, Broken Hill. Chemical analysis of Hoganite gave (wt%) C 23.85; H 3.95; Cu 31.6; Fe 0.4; O (by difference) 40.2, yielding an empirical formula of $C_4H_{7.89}O_{5.07}Cu_{1.00}Fe_{0.01}$ [9]. The simplified formula is $C_4H_8O_5Cu$ or $Cu(CH_3COO)_2 \cdot H_2O$, the mineral being identical to the synthetic compound of the same formula. All subsequent analyses were undertaken on the mineral Hoganite

X-ray diffraction

X-ray diffraction (XRD) patterns were recorded using $CuK\alpha$ radiation ($n = 154.18$ pm) on a Philips PANalytical X-Pert PRO diffractometer operating at 45 kV and 35 mA with 0.125° divergence slit, 0.25° anti-scatter slit, between 3 and 75° (2θ) at a step size of 0.02° .

Thermal Analysis

Thermal decomposition of the mineral was carried out in a TA® Instruments Incorporated high-resolution thermogravimetric analyzer (series Q500) in a flowing nitrogen atmosphere (80 cm³/min). Approximately 25 mg of sample was heated in an open platinum crucible at a rate of 6.0 °C/min up to 1000 °C, incorporating a controlled rate thermal analysis program. The TGA instrument was coupled to a Balzers (Pfeiffer) mass spectrometer for gas analysis. Only selected gases were analyzed.

Infrared spectroscopy

Infrared spectra were obtained using a Nicolet Nexus 870 FTIR spectrometer with a smart endurance single bounce diamond ATR cell. Spectra over the 4000 – 525 cm⁻¹ range were obtained by the co-addition of 64 scans with a resolution of 4 cm⁻¹ and a mirror velocity of 0.6329 cm/s. Spectral manipulation such as baseline adjustment, smoothing and normalisation was performed using the GRAMS® software package (Galactic Industries Corporation, Salem, NH, USA).

Near-infrared spectroscopy

Near infrared spectra were collected on a Nicolet Nexus FT-IR spectrometer with a Nicolet Near-IR Fibreport accessory. A white light source was used, with a quartz beam splitter and TEC NIR InGaAs detector. Spectra were obtained from $11\ 000$ to 4000 cm⁻¹ by the co-addition of 128 scans at a resolution of 8 cm⁻¹. A mirror velocity of 1.2659 cm/s was used. The spectra were transformed using the Kubelka-Munk algorithm to provide spectra for comparison with absorption spectra.

Spectral manipulation such as baseline adjustment, smoothing and normalisation were performed using the Spectralcalc software package GRAMS. Band component analysis was undertaken using the Jandel 'Peakfit' software package which enabled the type of fitting function to be selected and allowed specific parameters to be fixed or varied accordingly. Band fitting was done using a Lorentz-Gauss cross-product function with the minimum number of component bands used for the fitting process. The Gauss-Lorentz ratio was maintained at values greater than 0.7 and fitting was

undertaken until reproducible results were obtained with squared correlations greater than 0.995.

Raman spectroscopy

The crystals of Hoganite were placed on the stage of an Olympus BHSM microscope, equipped with 10x and 50x objectives. The microscope is part of a Renishaw 1000 Raman microscope system, which also includes a monochromator, a filter system and a charge coupled device (CCD). Raman spectra were excited by a double Nd-YAG laser (532 nm) at a resolution of 2 cm^{-1} in the range between 100 and 4000 cm^{-1} . Repeated acquisitions using the highest magnification were accumulated to improve the signal to noise ratio. Spectra were calibrated using the 520.5 cm^{-1} line of a silicon wafer. Previous studies by the authors provide more details of the experimental techniques [12, 13]. Spectral manipulation such as baseline adjustment, smoothing and normalisation was performed using the GRAMS® software package.

Scanning electron microscopy (SEM)

Samples were prepared for SEM by placement of a small amount of the calcined product on to an aluminium stub with the aid of double sided carbon tape. The samples were then coated with a thin layer of carbon to reduce charging during analysis. Secondary electron images were obtained using an FEI Quanta 200 scanning electron microscope. Elemental sample analysis was undertaken as required using energy dispersive X-ray (EDX) microanalysis.

Results and discussion:

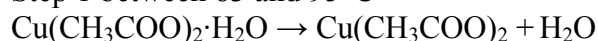
X-ray diffraction

X-Ray diffraction of the obtained mineral was undertaken (Figure 1(a)) to confirm its identity as copper acetate monohydrate. From the XRD spectrum we see the sample obtained is a near perfect match to the copper acetate hydrate reference pattern (27-145). Both the copper acetate and Hoganite compounds belong to the monoclinic crystal system. Hoganite has cell parameters of $a = 13.845$, $b = 8.528$ and $c = 13.197$, whilst the reference pattern copper acetate hydrate has cell parameters of $a = 13.863$, $b = 8.558$ and $c = 13.171$ which are very similar. The crystal structure of the mineral Hoganite is shown in Figure 1(b) clearly showing the relative spatial orientation of the water, acetate and copper groups.

Thermogravimetric analysis:

Thermogravimetric analysis of Hoganite and the mass spectrum of the evolved gases upon decomposition are shown below in Figures 2(a) and (b) respectively. The thermogravimetric (TG) and differential thermogravimetric (dTG) curves, shown in figure 2(a), show two distinct mass loss steps. The mass loss step between $83\text{ }^{\circ}\text{C}$ and $95\text{ }^{\circ}\text{C}$ is most likely due to the loss of the single molecule of water attached to the monohydrated acetate. This claim is supported by peaks in the mass spectrum between $82\text{ }^{\circ}\text{C}$ and $96\text{ }^{\circ}\text{C}$, for the 18 m/z ratio curve which is indicative of water. The mass loss of 9.4% also correlates well with the expected 9.0% mass loss for a single molecule of water, as is shown in the equation for mass loss step 1.

Step 1 between 83 and 95°C



The major mass loss of 58.6% at 222°C is attributed to the loss of the acetate anion as gaseous carbon dioxide and water. This theory is supported by peaks in the mass spectrum for mass to charge ratios of 44 and 18 (figure 2(b)). Quite clearly the equation for step 2 is not balanced with respect to the oxygen, as the apparatus may have been sucking in a small amount of air which was confirmed by the nature of the 32 m/z curve. The nitrogen used may also have contained a small amount of oxygen which is known to be inherently difficult to eliminate.

Step 2 at 222°C



X-ray diffraction of the TGA residues was also performed (figure 3) and revealed that the predominant copper oxide phase was cuprite (Cu_2O) with a very small amount of tenorite (CuO) present as well. It is quite evident that there is only a very small amount of tenorite in the residue and that the copper(I) oxide is being converted to the more stable copper(II) oxide. Thus for simplicity we have only indicated Copper(I) oxide as the final product in the decomposition reactions of hoganite shown previously.

Scanning electron microscope images of the TGA residues (figure 4(a)) were also acquired along with EDX analysis of the residual powder. There is thought to be a possibility that the copper acetate mineral may form copper oxide nanotubes or other nanostructures upon heating. Such nanostructures may be possible as the copper acetate contains both a metallic copper catalyst and acetate molecules which may act to provide the framework for such nanostructures. Unfortunately, analysis of the calcined product only illustrated the presence of a residual copper oxide (determined by EDX analysis (figure 4(b))) in the form of a typical high surface area sintered metal oxide. No interesting nanostructured materials were found in the residual powder.

Near-Infrared Spectroscopy

For the mineral Hoganite, the NIR spectrum consists of both O-H vibrations resulting from water units and C-H vibrations from the methyl group of the acetate anion. The spectrum has been divided into three regions being; the first fundamental O-H overtones (Figure 5(a)), O-H and C-H overtones (Figure 5(b)) and the O-H and C-H combination bands (Figure 5(c)). Results of band component analysis for the NIR, IR and Raman spectra are shown in Table 1.

The first fundamental overtone region shown in Figure 5(a) ($6200\text{-}7500\text{ cm}^{-1}$) is due to overtones of the water O-H stretching vibrations evident in the infrared spectrum. The NIR bands that were resolved at $6939, 6856, 6723, 6441\text{ cm}^{-1}$ are most likely due to overtones of the mid-IR bands that are present at $3471, 3427, 3368$ and 3210 cm^{-1} due to the close match observed from simply doubling these bands. The NIR spectrum of the water, O-H, and methyl, C-H, overtones is shown in Figure 5(b) in the region from $5500\text{-}6100\text{ cm}^{-1}$. The two well resolved bands at 6001 and 5943 cm^{-1}

are likely to be the first overtone of the two small C-H stretching vibrations present in the mid IR and Raman spectra at ~ 2988 and ~ 2942 cm^{-1} . Whilst the four bands that are present at 5800, 5719, 5654 and 5630 cm^{-1} are due to water overtones and are typical of a water type spectrum for minerals [14].

Figure 5(c) shows the region of the NIR spectrum from 4075-5450 cm^{-1} which is dominated by combination bands involving O-H stretching and deformations as well as C-H stretching and deformations. The complex series of bands present from 4600-4300 cm^{-1} are due to the combination of Raman active bands present between 3024-2862 cm^{-1} (attributed to C-H stretching vibrations) with bands between 1360-1450 cm^{-1} (attributed to C-H deformations). The number of resolved bands in this region simply demonstrates the complexity of the hoganite molecular structure. Finally the bands present at 5218, 5130, 5022 and 4861 cm^{-1} in the NIR spectrum are due to combinations of the O-H stretching vibrations evident in the mid-IR between 3210-3528 cm^{-1} with the weak O-H deformations which were observed in the Raman spectrum between 1640-1670 cm^{-1} .

Infrared spectroscopy

The infrared spectrum of copper acetate hydrate at room temperature is provided in Figures 6(a)-(c). Figure 6(a) shows the infrared spectrum in the region from 2850-3700 cm^{-1} . The spectrum is dominated by three large peaks at 3471, 3368 and 3269 cm^{-1} which are due to O-H stretching vibrations from the single molecule of water that is associated with the acetate anion. Quite clearly there are at least three different environments of the O-H units leading to three intense bands with variation in the location of the stretching vibrations due to differences in the strength of the hydrogen bonds. There are also two small broad peaks present at 2942 cm^{-1} and 2988 cm^{-1} which are commonly observed in any acetate spectra and are due to the A_1 $\nu(\text{CH})$ stretch and the B_1 $\nu(\text{CH})$ stretching vibrations [15].

Figure 6(b) shows the infrared spectrum in the region from 1200-1700 cm^{-1} . A small sharp peak is present at 1354 cm^{-1} which is due to the A_1 $\delta(\text{CH}_3)$ rocking vibration. Upon band component analysis of the peaks around 1430 cm^{-1} , three bands were found. The band at 1418 cm^{-1} is due to the A_1 (COO) stretching vibration, the small broad band at 1439 cm^{-1} is due to the B_1 $\delta(\text{CH}_3)$ deformation and finally the intense band at 1443 cm^{-1} is due to the B_2 $\delta(\text{CH}_3)$ deformation [16]. There is also one other very intense peak in the spectrum present at 1598 cm^{-1} which we attribute to the B_1 (COO) asymmetric stretching vibration of the acetate[5].

Figure 6(c) shows the low wave number region from 575-1075 cm^{-1} . The infrared spectrum in this region is dominated by two intense bands at 627 cm^{-1} and 687 cm^{-1} which are attributed to B_2 $\pi(\text{COO})$ rocking and A_1 $\delta(\text{OCO})$ deformation of the acetate anion [5, 15]. There are two other bands in this region of the spectrum at 1033 cm^{-1} and 1051 cm^{-1} which can be attributed to the B_1 and B_2 $\rho_\gamma(\text{CH}_3)$ rocking vibration. All band assignments in the infrared correlate well with other values published on various other metal acetates [5].

Raman spectroscopy

The Raman spectrum of hoganite displaying the C-H and O-H stretching region is shown in the Figure 7(a). Quite clearly we see a single, weak band at 3478 cm^{-1} which we attribute to the O-H stretching from the water molecule. There are a number of sharp, intense bands at 2941 , 2989 and 3024 cm^{-1} due to C-H stretching within the methyl group. More specifically the vibrational bands at 3024 and 2989 cm^{-1} are due to B_1 and B_2 $\nu(\text{CH})$ stretching whilst the band at 2941 cm^{-1} is due to the A_1 C-H symmetric stretching vibration [16].

When salts of carboxylic acids such as acetic are formed the C=O and C-O bonds are replaced by two equivalent $\text{C}=\text{O}$ bonds with a bond order of 1.5 [3, 17-20]. These two $\text{C}=\text{O}$ bonds interact in-phase and out of phase to give two bands: the asymmetric stretching vibration which is intense in the infrared spectrum but relatively weak in the Raman spectrum, and a symmetric stretching band which is weak in intensity in the infrared spectrum but strong and polarised in the Raman spectrum [5]. These two vibrations are normally found in the $1540\text{-}1650$ and $1360\text{-}1450\text{ cm}^{-1}$ regions respectively [18, 20]. The Raman spectrum of the $\text{C}=\text{O}$ stretching region of the acetates is shown in Figure 7(b), in the region of $1325\text{-}1500\text{ cm}^{-1}$.

We quite clearly see three distinct peaks upon band component analysis in the region from $1410\text{-}1450\text{ cm}^{-1}$, which we can attribute to the symmetric stretching vibrations of the $\text{C}=\text{O}$ bond and deformations of the methyl substituent. The band at 1449 cm^{-1} is due to the B_2 $\delta(\text{CH}_3)$ deformation, whilst the band at 1440 cm^{-1} is attributed to the A_1 $\nu(\text{COO})$ stretching vibration and finally the band at 1418 cm^{-1} is attributed to the B_1 $\delta(\text{CH}_3)$ deformation [5]. The asymmetric stretching vibrations could not be resolved from the background noise in the region from $1540\text{-}1650\text{ cm}^{-1}$ in the Raman spectrum, though was observed to be a very intense band in the infrared at 1598 cm^{-1} , as stated earlier. Figure 7(b) also shows a clearly resolved A_1 methyl (HCH) deformation at 1360 cm^{-1} , which is to be expected in the Raman spectrum of a metal acetate [5].

Figure 7(c) depicts the $150\text{-}1000\text{ cm}^{-1}$ region of the Raman spectrum for hoganite. We see two sets of peaks at 948 and 938 cm^{-1} and 703 and 684 cm^{-1} which are attributed to the A_1 $\nu(\text{CC})$ stretch and the A_1 $\delta(\text{OCO})$ deformation on the acetate anion. Interestingly, a well resolved split of each of these vibrations can be observed, leading us to believe that the acetate anion is present in two different conformations in the crystal structure

Conclusions

A comprehensive spectroscopic and thermal analysis of the mineral Hoganite was undertaken. Vibrational bands due to the acetate anion have been assigned in Raman, IR and NIR spectroscopic techniques. Thermal analysis of the mineral revealed two major mass loss steps, the first step at around 90°C is due to the loss of the water molecule whilst the major mass loss step at 222°C is thought to be the result of the loss of the acetate anion as carbon dioxide and water vapour. The resulting sintered metal oxide formed after TGA was comprised mainly of a Copper(I) oxide phase, as confirmed by X-ray diffraction and EDX analysis.

Acknowledgments

The financial and infra-structure support of the Queensland University of Technology Inorganic Materials Research Program of the School of Physical and Chemical Sciences is gratefully acknowledged. The Australian Research Council (ARC) is thanked for funding.

References

- [1]. G. S. Raghuvanshi, M. Pal, M. B. Patel and H. D. Bist, *Journal of Molecular Structure* 101 (1983) 7.
- [2]. G. S. Raghuvanshi, D. P. Khandelwal and H. B. Bist, *Spectrochimica Acta Part A: Molecular and Biomolecular Spectroscopy* 37 (1981).
- [3]. K. Ito and H. J. Bernstein, *Can. J. Chem.* 34 (1956) 170.
- [4]. L. H. Jones and E. J. McLaren, *Journal of Chemical Physics* 22 (1954) 1796.
- [5]. R. L. Frost and J. T. Kloprogge, *Journal of Molecular Structure* 526 (2000) 131.
- [6]. G. S. Raghuvanshi, D. P. Khandelwal and H. D. Bist, *Spectrochimica Acta, Part A: Molecular and Biomolecular Spectroscopy* 41A (1985) 391.
- [7]. R. I. Bickley, H. G. M. Edwards, S. J. Rose and R. Gustar, *Journal of Molecular Structure* 238 (1990) 15.
- [8]. Z. Nickolov, I. Ivanov, G. Georgiev and D. Stoilova, *Journal of Molecular Structure* 377 (1996) 13.
- [9]. D. E. Hibbs, U. Kolitsch, P. Leverett, J. L. Sharpe and P. A. Williams, *Mineralogical Magazine* 66 (2002) 459.
- [10]. K. Zhang, J. Hong, G. Cao, D. Zhan, Y. Tao and C. Cong, *Thermochimica Acta* 437 (2005) 145.
- [11]. A. Y. Obaid, A. O. Alyoubi, A. A. Samarkandy, S. A. Al-Thabaiti, S. S. Al-Juaid, A. A. El-Bellihi and E.-H. M. Deifallah, *Journal of Thermal Analysis and Calorimetry* 61 (2000) 985.
- [12]. R. L. Frost, W. N. Martens and P. A. Williams, *Journal of Raman Spectroscopy* 33 (2002) 475.
- [13]. R. L. Frost, W. Martens, J. T. Kloprogge and P. A. Williams, *Journal of Raman Spectroscopy* 33 (2002) 801.
- [14]. R. L. Frost, K. L. Erickson, O. Carmody and M. L. Weier, *Spectrochimica Acta Part A: Molecular and Biomolecular Spectroscopy* 61 (2005) 749.
- [15]. K. Nakamoto, *Infrared Spectra of Inorganic and Coordination Compounds*, John Wiley & Sons, New York, 1963.
- [16]. V. Koleva, *Croatica chemica acta* 78 (2005) 581.
- [17]. E. Spinner, *Journal of the Chemical Society, Abstracts* (1964) 4217.
- [18]. N. B. Colthup, L. H. Daly and S. E. Wiberly, *Introduction to infrared and Raman spectroscopy*, 3 ed., Academic, New York, 1974.
- [19]. J. Semmler, D. E. Irish and T. Ozeki, *Geochimica et Cosmochimica Acta* 54 (1990) 947.
- [20]. D. Lin-Vien, N. B. Colthup, W. G. Fateley and J. G. Graselli, *The handbook of infrared and Raman characteristic frequencies of organic molecules*, Academic, SanDiego, 1991.

List of Tables:

Table 1: NIR, IR and Raman combined spectroscopic analysis data table

Near Infrared			Infrared			Raman		
Center (cm ⁻¹)	FWHM (cm ⁻¹)	%	Center (cm ⁻¹)	FWHM (cm ⁻¹)	%	Center (cm ⁻¹)	FWHM (cm ⁻¹)	%
7403	44.8	0.2	3528	86.8	3.8			
7343	36.0	0.0	3471	66.1	10.5	3478	54.8	2.0
7268	87.1	0.4	3427	56.3	3.1			
7023	38.9	0.1	3368	60.2	13.3			
6939	102.9	1.4	3323	40.9	1.4			
6856	106.8	3.9	3269	42.8	4.9			
6723	193.3	5.5	3210	127.4	3.4			
6441	235.2	3.9				3024	17.2	7.3
6308	87.6	0.5	2988	17.3	0.2	2989	18.5	3.0
6001	27.7	2.0	2942	17.4	0.2	2941	16.6	19.0
5943	46.4	2.5				2922	71.3	8.7
5800	92.3	6.1				2862	29.5	1.7
5719	60.9	1.9				2788	20.6	0.3
5654	58.5	1.3	2364	18.2	0.3			
5630	78.3	1.7	2335	38.8	0.7			
5378	41.1	0.2	1650	10.9	0.4			
5359	28.6	0.1	1598	41.2	19.0			
5218	90.6	7.1	1554	49.5	4.8			
5178	53.3	3.5	1504	39.1	1.6			
5130	61.1	9.2	1443	23.8	5.7	1449	13.9	2.7
5075	45.9	1.4	1439	24.8	1.0	1440	12.6	5.7
5029	109.3	14.3	1418	26.3	9.9	1418	12.1	4.4
4861	109.0	1.5	1397	95.0	7.8			
4651	23.9	0.2	1354	7.2	0.6	1360	7.6	1.2
4616	53.5	0.8	1051	11.9	0.6			
4560	49.4	1.7	1033	11.3	1.0			
4504	132.6	3.9				948	4.9	7.5
4436	35.8	4.3				938	6.5	2.1
4412	108.0	10.5				703	9.2	4.3
4372	38.5	3.2	687	19.8	4.1	684	9.0	1.2
4329	27.9	2.8	664	25.5	0.5			
4300	31.1	1.0	627	11.6	0.9			
4201	37.1	0.4	547	70.0	0.2			
4161	45.3	0.8				322	14.2	13.5
4123	37.6	0.2				297	25.3	8.5
4048	18.8	0.7				266	7.5	0.5
4027	26.2	0.6				252	8.6	1.7
						230	15.8	1.1
						212	9.7	3.2
						184	15.1	0.8

Table 1: NIR, IR and Raman combined spectroscopic analysis data table

List of Figures:

Figure 1(a): XRD of Hoganite
(b): Crystal structure of Hoganite

Figure 2(a): TG analysis of Hoganite
(b): MS analysis of Hoganite

Figure 3: XRD of TGA residues

Figure 4(a): SEM image of calcined Hoganite
4(b): EDX spectrum of calcined Hoganite surface

Figure 5(a): NIR spectrum of Hoganite: $6200\text{-}7500\text{cm}^{-1}$
(b): NIR spectrum of Hoganite: $5500\text{-}6100\text{cm}^{-1}$
(c): NIR spectrum of Hoganite: $4075\text{-}5450\text{cm}^{-1}$

Figure 6(a): Infrared spectrum of Hoganite: $2850\text{-}3700\text{cm}^{-1}$
(b): Infrared spectrum of Hoganite: $1200\text{-}1700\text{cm}^{-1}$
(c): Infrared spectrum of Hoganite: $575\text{-}1075\text{cm}^{-1}$

Figure 7(a): Raman spectrum of Hoganite: $2750\text{-}3600\text{cm}^{-1}$
(b): Raman spectrum of Hoganite: $1325\text{-}1500\text{cm}^{-1}$
(c): Raman spectrum of Hoganite: $150\text{-}1000\text{cm}^{-1}$

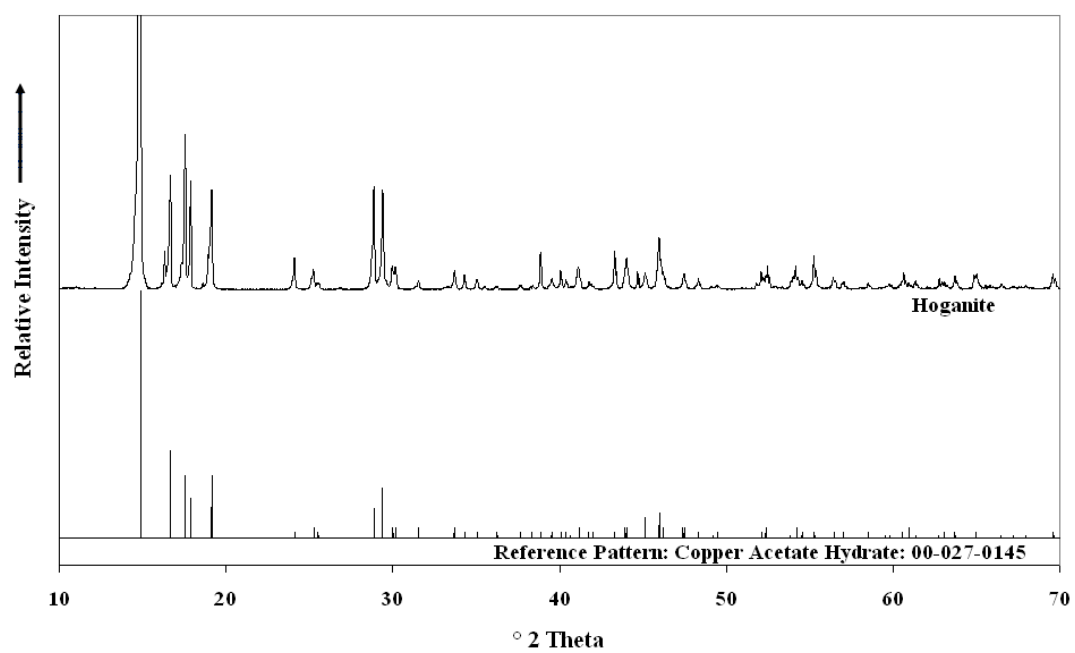


Figure 1(a): XRD of Hoganite and the reference pattern of copper acetate hydrate

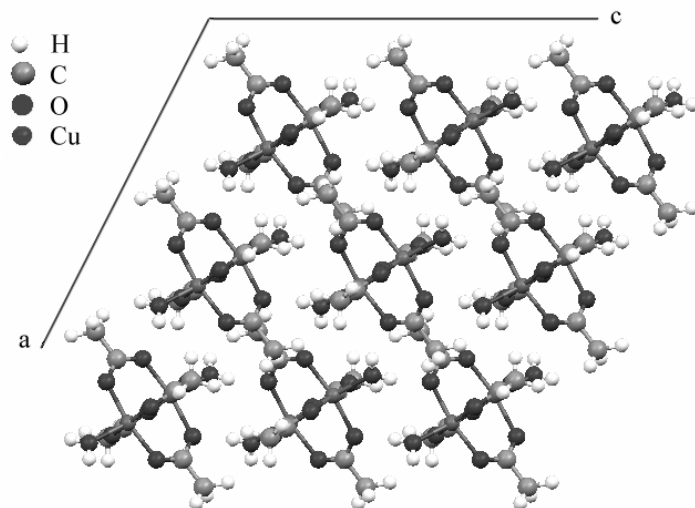


Figure 1(b) Crystal structure of Hoganite.

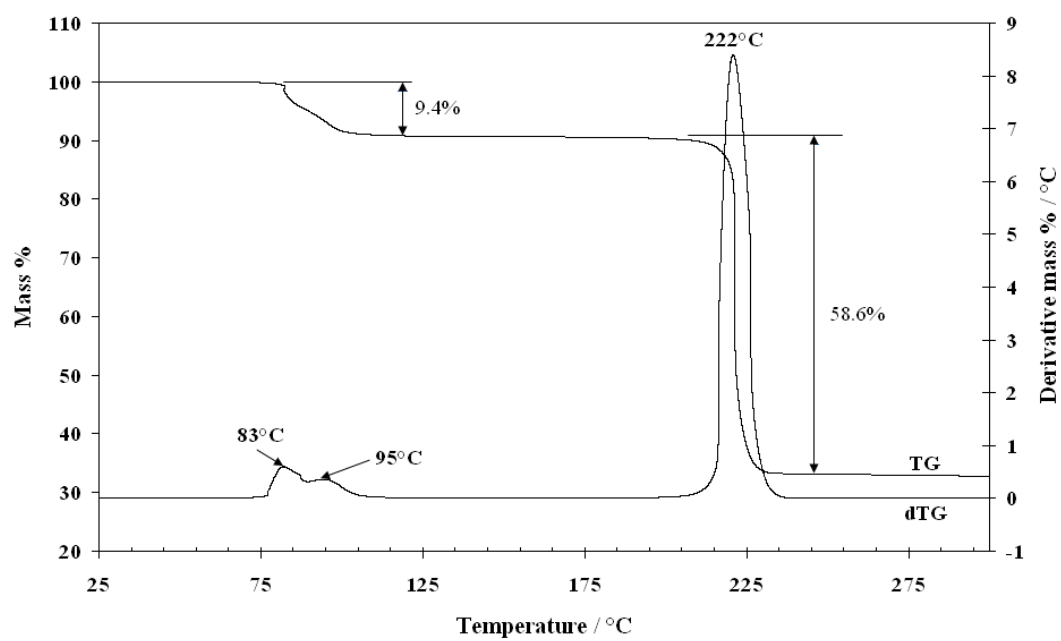


Figure 2(a): TG of Hoganite

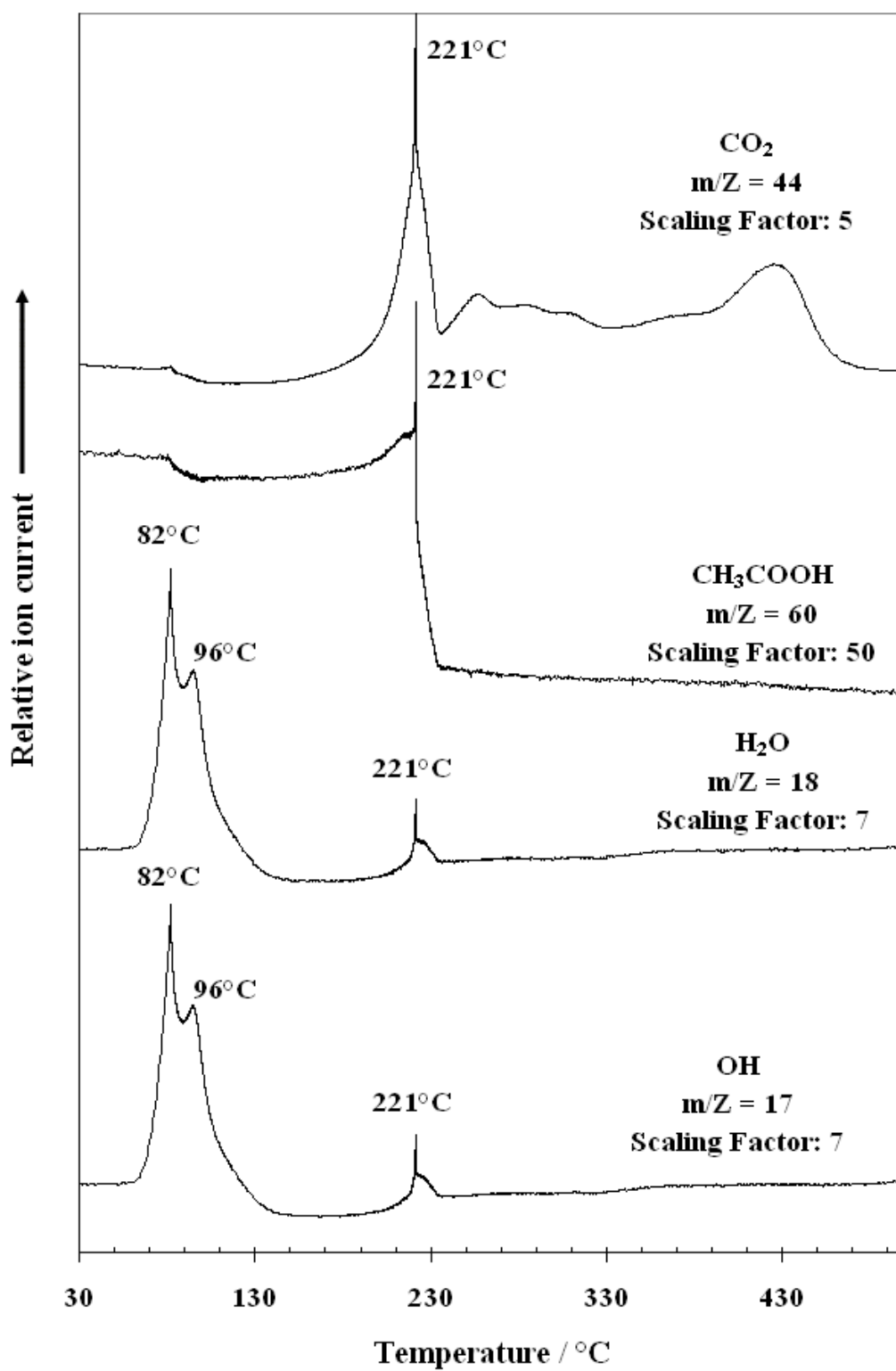


Figure 2(b): MS of Hoganite

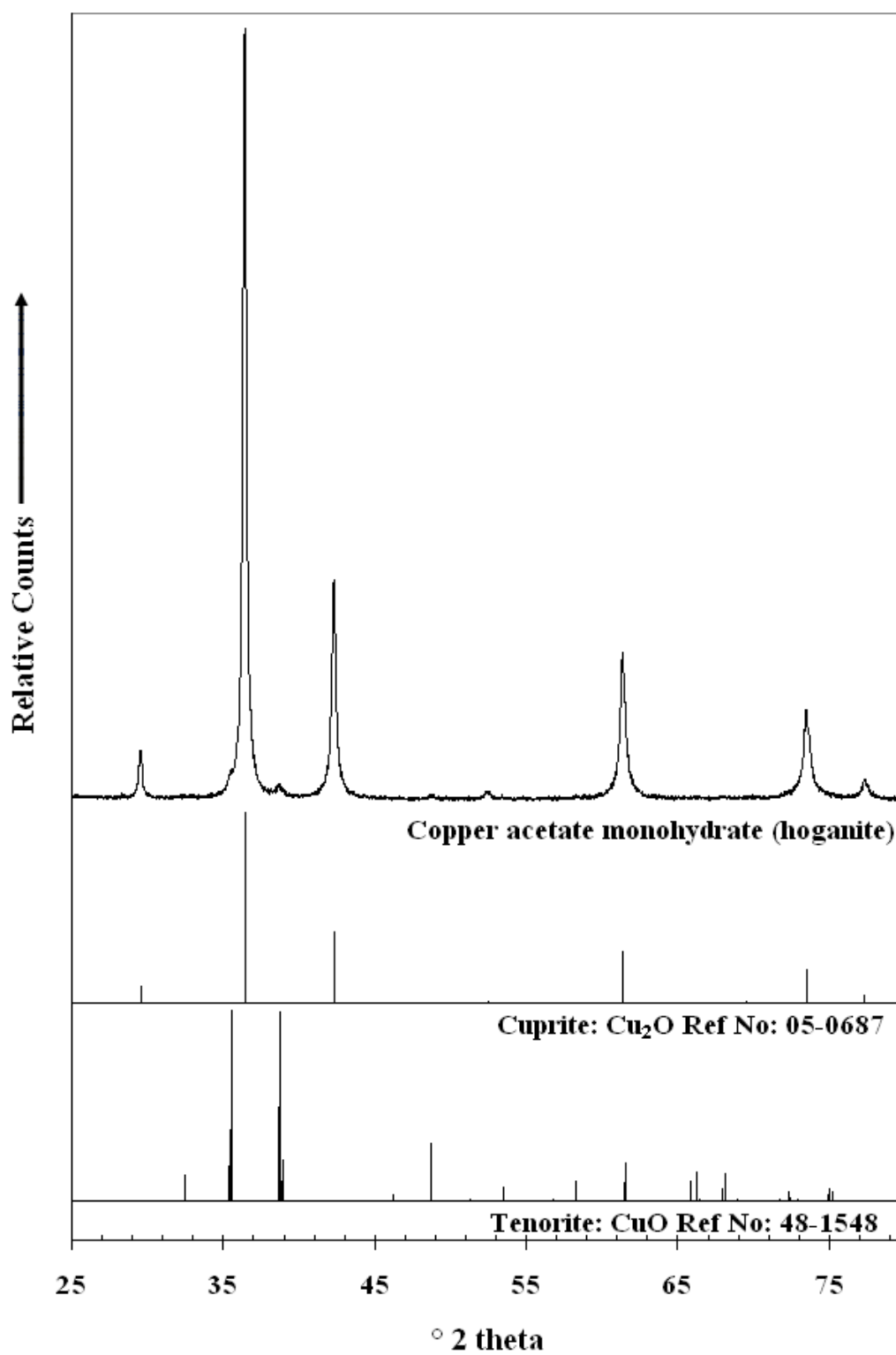


Figure 3: XRD of TGA residues

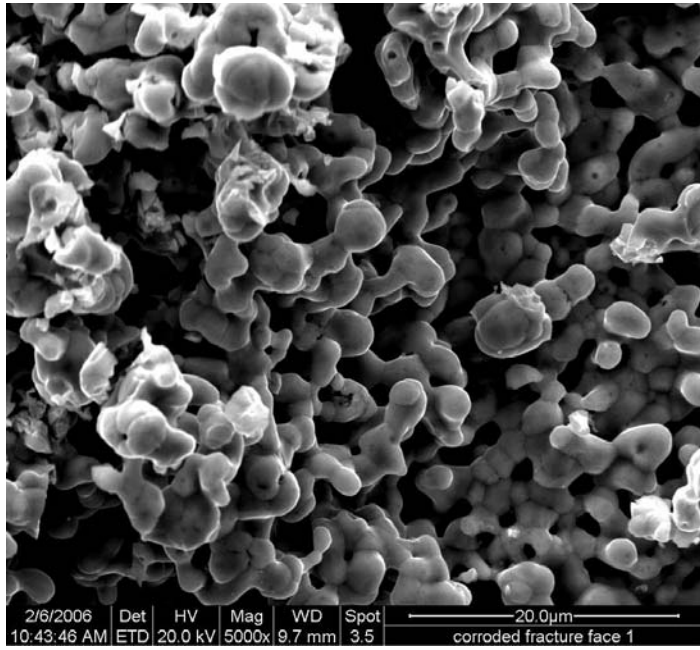


Figure 4(a): SEM image of calcined Hoganite

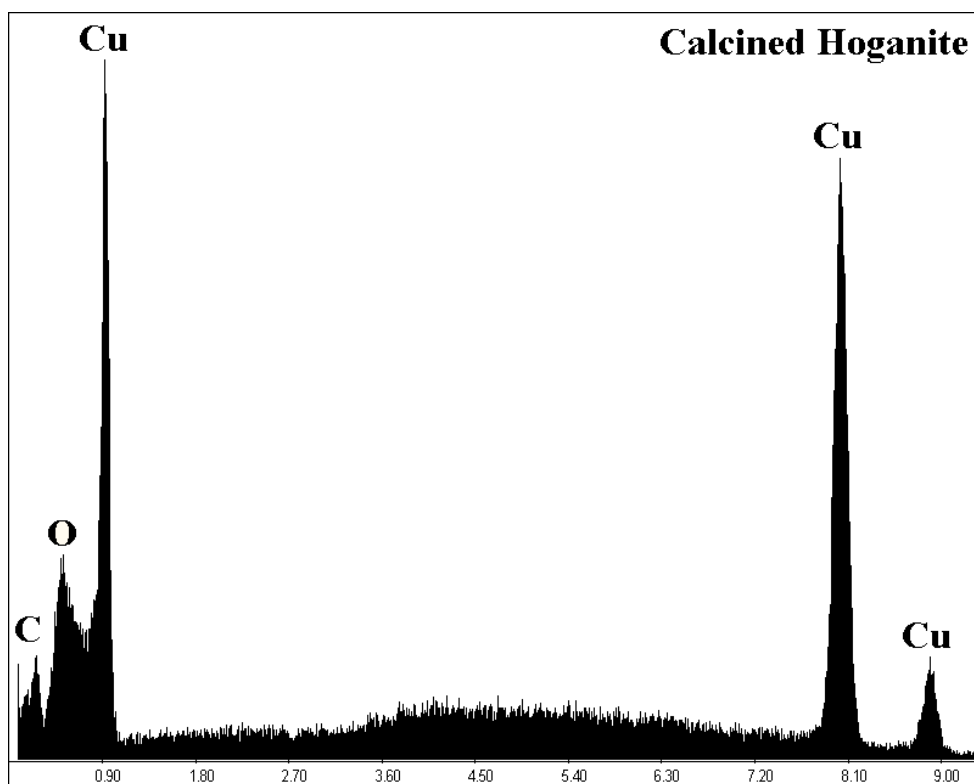


Figure 4(b): EDX analysis of calcined Hoganite surface.

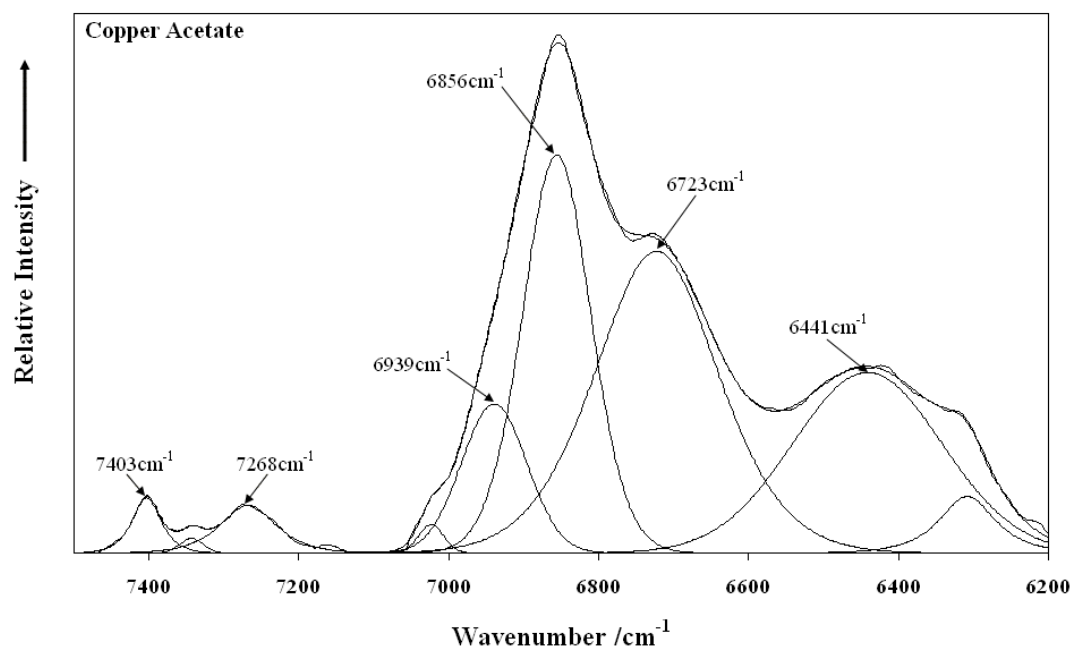


Figure 5(a): NIR spectrum of Hoganite: 6200-7500cm⁻¹

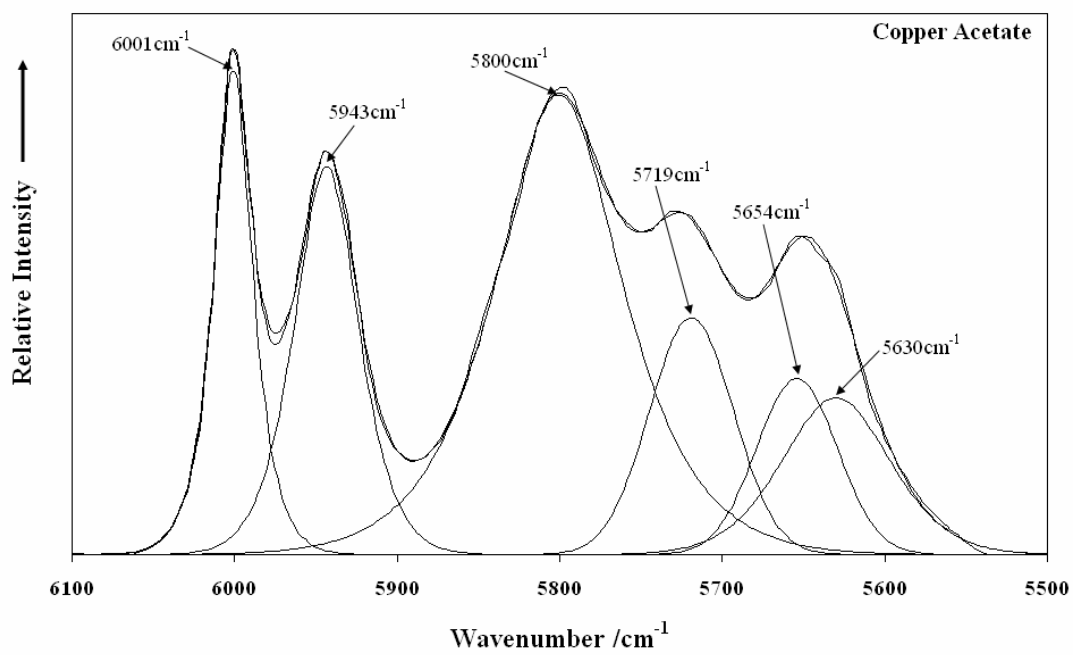


Figure 5(b): NIR spectrum of Hoganite: 5500-6100 cm^{-1}

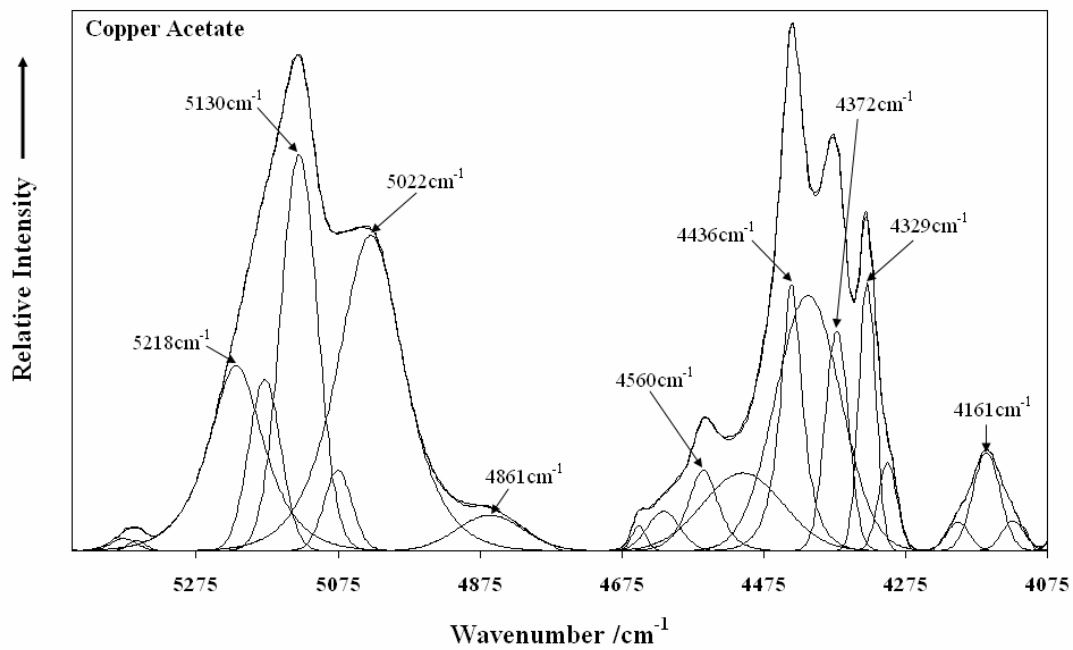


Figure 5(c): NIR spectrum of Hoganite: 4075-5450cm⁻¹

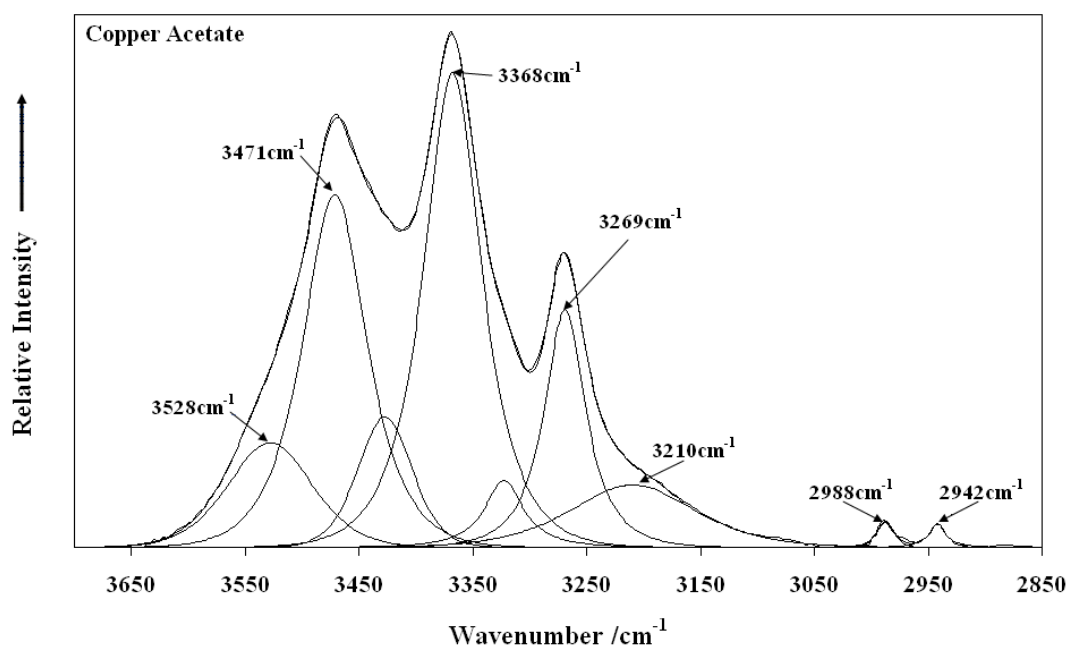


Figure 6(a): Infrared spectrum of Hoganite: 2850-3700 cm^{-1}

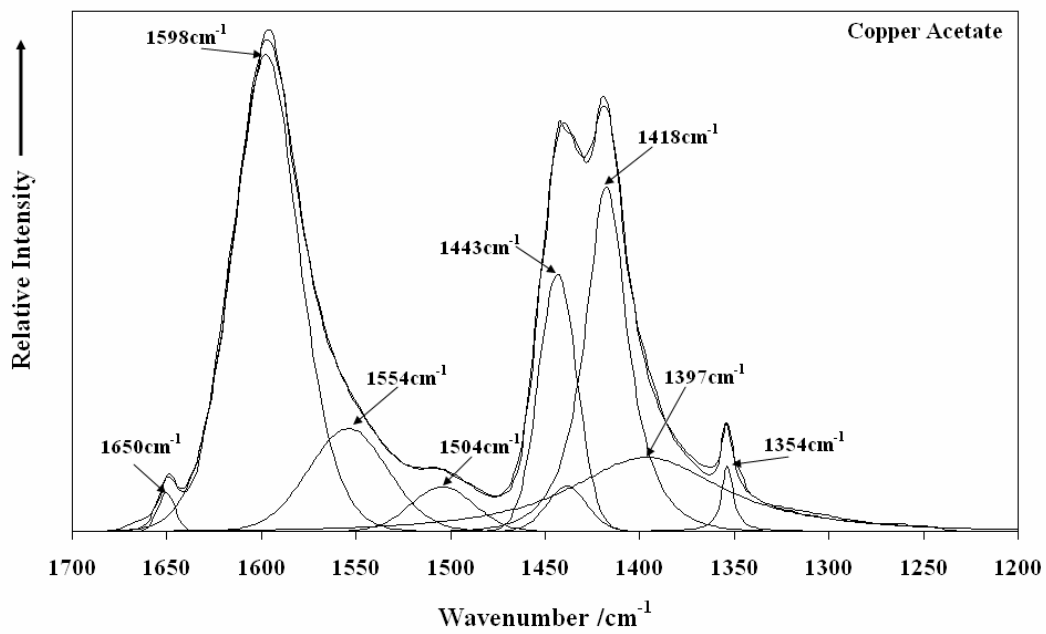


Figure 6(b): Infrared spectrum of Hoganite: $1200\text{-}1700\text{cm}^{-1}$

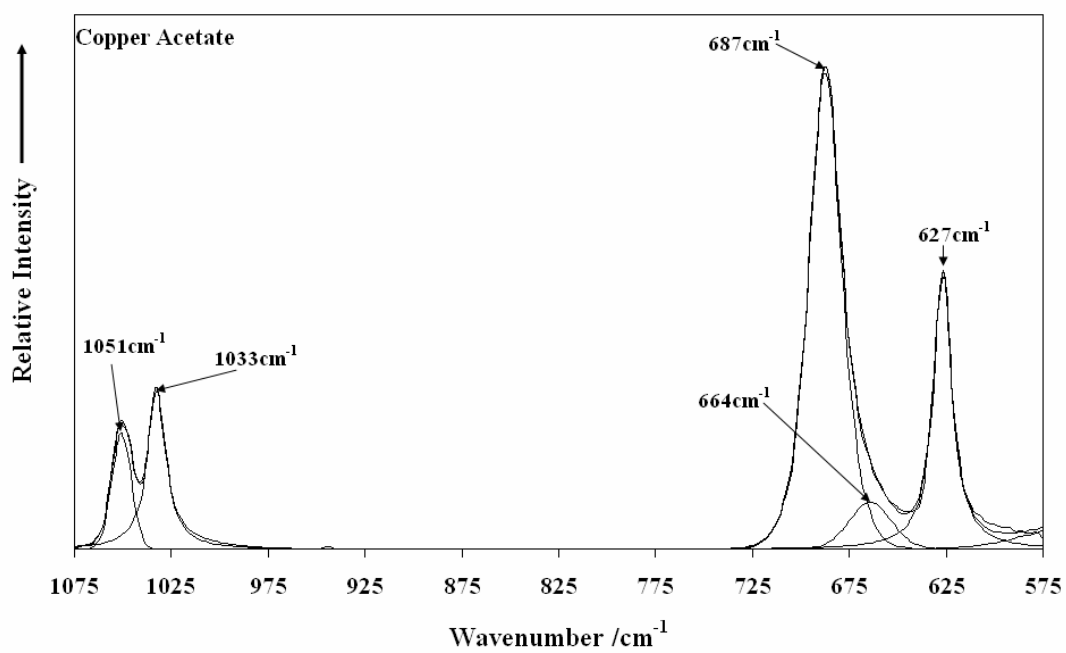


Figure 6(c): Infrared spectrum of Hoganite: 575-1075cm⁻¹

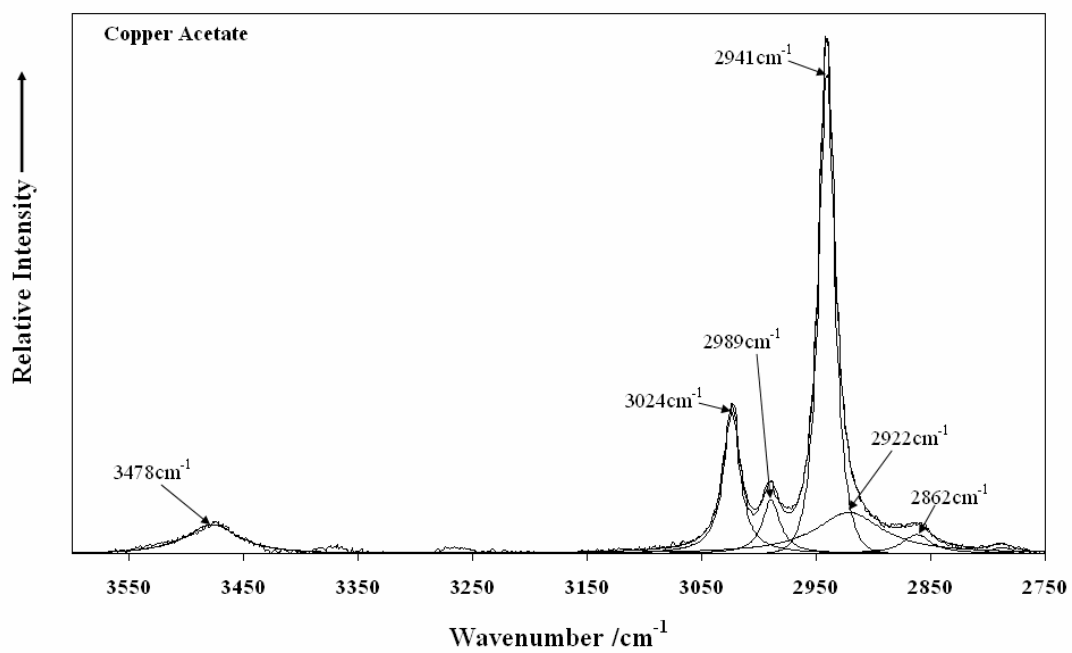


Figure 7(a): Raman spectrum of Hoganite: 2750-3600 cm^{-1}

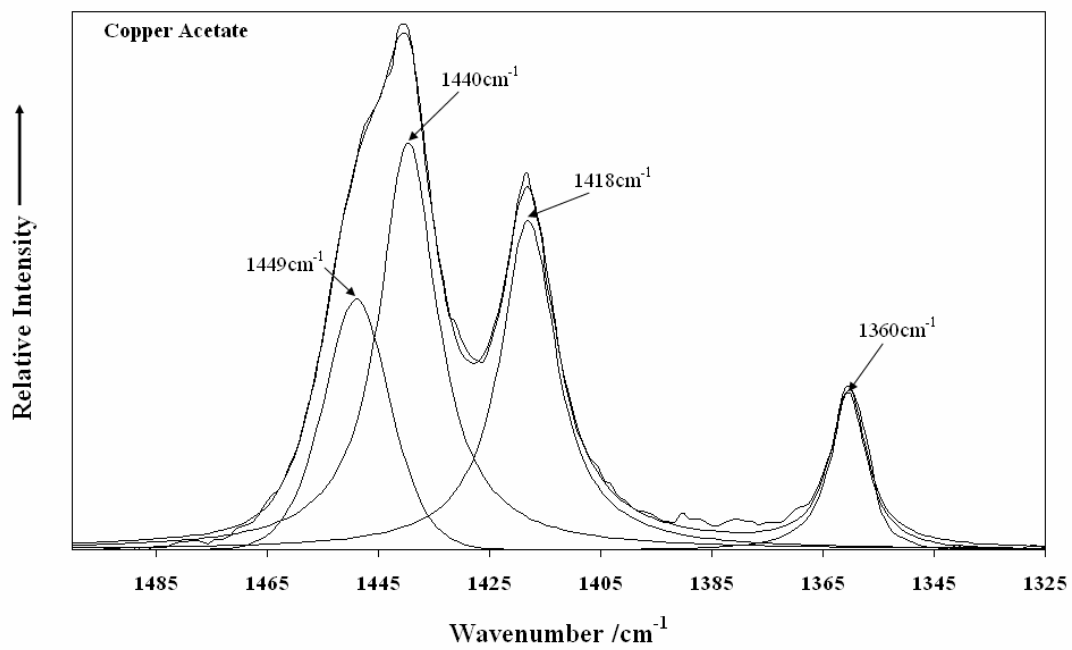


Figure 7(b): Raman spectrum of Hoganite: 1325-1500cm⁻¹

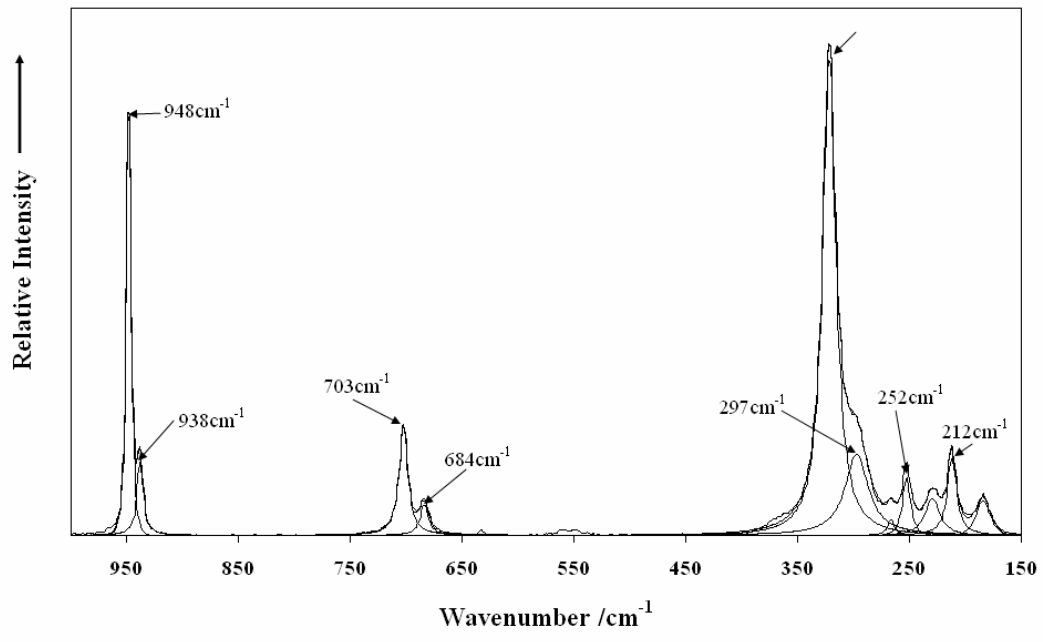


Figure 7(c): Raman spectrum of Hoganite: 150-1000cm⁻¹